

Electronic Supplementary Information

Pressure-Dependent Kinetics of *o*-Xylene Reaction with OH Radical

Yan Li,¹Xuan Guo,^{1,2} Rui Ming Zhang,¹ Hui Zhang,¹ Xin Zhang,^{2,*} and Xuefei Xu^{1,*}

¹*Center for Combustion Energy, Department of Energy and Power Engineering, and Key Laboratory for Thermal Science and Power Engineering of Ministry of Education, Tsinghua University, Beijing 100084, China*

²*State Key Laboratory of Chemical Resource Engineering, Institute of Materia Medica, College of Science, Beijing University of Chemical Technology, Beijing, 100029, P.R. China*

*Corresponding authors.

E-mail addresses: xuxuefei@tsinghua.edu.cn (X.X.).

The Calculation and Usage of Specific-Reaction-Parameter (SRP) scaling factor λ^{SRP} in This Work.

Usually the standard scaling factors parametrized to obtain accurate zero point energies (ZPE) in the F38/10 database¹ are good enough for the stable molecules, but they fail to correct the strong high-frequency anharmonicity of transition states or pre-reactive complexes for some reactions.²⁻⁴ Therefore, for the lowest-energy structures of transition states of the six reaction channels, we firstly used hybrid⁵ degeneracy-corrected⁶ second-order⁷⁻⁹ vibrational perturbation theory (HDCVPT2) to calculate the anharmonic vibration frequencies to get anharmonic ZPEs, and then we employed the method proposed by Zheng et al.³ to determine the corresponding specific-reaction-parameter scaling factor by $\lambda^{\text{SRP}} = \lambda^{\text{Anh}}\lambda^{\text{H}}$, where λ^{Anh} is the ratio of the computed anharmonic ZPE to the harmonic ZPE, and λ^{H} correcting for the inexactness of the model chemistry is determined by reproducing the accurate harmonic frequencies in the F38/10 database. These scaling factors of frequencies are also used in torsional anharmonicity and dynamics calculations.

We calculated the frequency scaling factors λ^{SRP} and λ^{STD} for the transition states of A1-A3 and B1-B3 reactions as shown in **Table S2**. In the calculations of λ^{Anh} , M08-HX/jul-cc-pVDZ and MPW1K¹⁰/MG3S were used for hydrogen abstraction (A1-A3) and OH addition reactions (B1-B3), respectively. From the table, we can see that the determined λ^{SRP} scaling factors for the transition states of hydrogen abstraction reactions are slightly smaller than the standard scaling factor λ^{STD} , while those of addition reactions are equal to the corresponding λ^{STD} factor, so we used λ^{SRP} only for the transition states of A1-A3 reactions. For other species (including all the reactants, complexes, transition states of B1-B3, and products), we used λ^{STD} to scale the harmonic frequencies.

Table S1 Calculated T_1 diagnostics by the CCSD/jul-cc-pVTZ//M08-HX/ma-TZVP method.

structure	T_1
$\cdot\text{OH}$	0.008
<i>o</i> -xylene	0.010
TS abstraction 1	0.021
TS abstraction 2	0.022
TS abstraction 3	0.022
$\cdot\text{CH}_2\text{C}_6\text{H}_4\text{CH}_3$	0.020
<i>o</i> -CH ₃ $\cdot\text{C}_6\text{H}_3\text{CH}_3$	0.013
<i>m</i> -CH ₃ $\cdot\text{C}_6\text{H}_3\text{CH}_3$	0.013
H ₂ O	0.009
TS addition 1	0.027
TS addition 2	0.026
TS addition 3	0.026
CH ₃ C ₆ H ₄ CH ₃ OH	0.016
<i>o</i> -CH ₃ C ₆ H ₄ (OH)CH ₃	0.016
<i>m</i> -CH ₃ C ₆ H ₄ (OH)CH ₃	0.016

Table S2 Scaling factors for transition states.

Reaction	Abstraction				Addition	
	methyl-	<i>o</i> -	<i>m</i> -	<i>ipso</i> -	<i>o</i> -	<i>m</i> -
λ^{STD}		0.979 ^a			0.983 ^b	
λ^{H}		0.988 ^a			0.995 ^b	
λ^{Anh}	0.988 ^a	0.989 ^a	0.987 ^a	0.988 ^c	0.987 ^c	0.987 ^c
$\lambda^{\text{SRP}} = \lambda^{\text{Anh}}\lambda^{\text{H}}$	0.977	0.978	0.975	0.983	0.983	0.983
λ^{ZPE} we choose	0.977	0.978	0.975	0.983	0.983	0.983

^a Calculated by M08-HX/jul-cc-pVDZ method.

^b Calculated by M08-SO/ma-TZVP method.

^c Calculated by MPW1K/MG3S method.

Table S3 Classical forward barrier heights (V_f^\ddagger), classical reverse barrier heights (V_r^\ddagger) and classical reaction energies (ΔV) (in kcal/mol) of A1-A3 hydrogen abstraction reactions and the mean unsigned deviations (MUD in kcal/mol) against the benchmark results obtained by CCSD(T)-F12b/jul-cc-pVTZ//M08-HX/ma-TZVP.

Method	Basis set	abs-methyl			abs- <i>o</i>			abs- <i>m</i>			MUD
		V_f^\ddagger	V_r^\ddagger	ΔV	V_f^\ddagger	V_r^\ddagger	ΔV	V_f^\ddagger	V_r^\ddagger	ΔV	
M06-2X	jul-cc-pVDZ	0.28	27.05	-26.77	3.92	10.59	-6.67	4.75	10.95	-6.20	1.17
M08-HX	jul-cc-pVDZ	1.14	28.64	-27.50	4.87	11.03	-6.16	5.69	11.40	-5.72	0.46
M08-SO	jul-cc-pVDZ	-0.16	26.80	-26.96	3.95	9.17	-5.22	4.86	9.58	-4.72	1.69
M05-2X	jul-cc-pVDZ	0.50	28.93	-28.43	4.18	9.60	-5.42	4.91	9.87	-4.95	1.07
MN12-SX	jul-cc-pVDZ	0.21	28.29	-28.08	5.09	12.49	-7.39	5.84	12.73	-6.89	0.78
MN12-L	jul-cc-pVDZ	0.91	28.16	-27.25	6.26	13.06	-6.80	7.14	13.57	-6.43	1.05
MN15-L	jul-cc-pVDZ	-0.26	27.43	-27.69	5.12	11.77	-6.65	6.20	12.51	-6.30	0.72
MPW1K	jul-cc-pVDZ	0.90	26.99	-26.09	5.43	9.58	-4.15	6.12	9.70	-3.59	1.58
M06-2X	ma-TZVP	1.03	27.26	-26.23	4.83	10.72	-5.89	5.67	11.08	-5.41	0.91
M08-HX	ma-TZVP	2.29	28.68	-26.39	6.27	10.94	-4.67	7.12	11.42	-4.29	1.14
M08-SO	ma-TZVP	0.95	27.37	-26.42	5.48	9.33	-3.85	6.44	9.82	-3.38	1.61
M05-2X	ma-TZVP	1.15	28.89	-27.74	5.07	9.44	-4.37	5.82	9.74	-3.92	1.13
MN12-SX	ma-TZVP	1.64	28.58	-26.94	6.59	11.94	-5.35	7.44	12.32	-4.88	0.92
MN12-L	ma-TZVP	2.34	28.37	-26.03	7.51	12.76	-5.25	8.44	13.39	-4.95	1.55
MN15-L	ma-TZVP	0.35	27.39	-27.05	5.56	11.26	-5.69	6.62	11.99	-5.37	0.78
MPW1K	ma-TZVP	1.70	27.32	-25.63	6.32	9.65	-3.33	7.01	9.79	-2.78	1.95
CCSD(T)-F12b	jul-cc-PVTZ	1.34	29.69	-28.35	5.28	11.59	-6.31	6.03	11.87	-5.84	0.00

All the energies are with ZPEs excluded and calculated using the structures optimized by M08-HX/ma-TZVP method.

Table S4 Classical forward barrier heights (V_f^\ddagger), classical reverse barrier heights (V_r^\ddagger) and classical reaction energies (ΔV) (in kcal/mol) of B1-B3 OH-addition reactions and the mean unsigned deviations (MUD in kcal/mol) against the benchmark results obtained by CCSD(T)-F12b/jul-cc-pVTZ//M08-HX/ma-TZVP.

Method	Basis set	add- <i>ipso</i>			add- <i>o</i>			add- <i>m</i>			MUD
		V_f^\ddagger	V_r^\ddagger	ΔV	V_f^\ddagger	V_r^\ddagger	ΔV	V_f^\ddagger	V_r^\ddagger	ΔV	
M06-2X	jul-cc-pVDZ	-2.65	20.73	-23.38	-2.65	19.71	-21.18	-0.62	21.06	-21.67	0.95
M08-HX	jul-cc-pVDZ	-2.74	20.10	-22.84	-2.74	19.66	-20.91	-0.50	20.88	-21.39	0.77
M08-SO	jul-cc-pVDZ	-4.88	19.05	-23.93	-4.88	18.80	-22.14	-2.55	20.19	-22.74	1.44
M05-2X	jul-cc-pVDZ	-3.58	20.93	-24.51	-3.58	19.63	-21.96	-1.53	21.02	-22.44	1.29
MN12-SX	jul-cc-pVDZ	-3.89	16.76	-20.65	-3.89	16.47	-19.14	-2.04	17.77	-19.81	1.52
MN12-L	jul-cc-pVDZ	-3.51	14.93	-18.45	-3.51	14.82	-16.62	-1.24	16.04	-17.14	2.77
MN15-L	jul-cc-pVDZ	-5.98	16.06	-22.04	-5.98	15.35	-19.26	-3.09	16.47	-19.52	2.31
MPW1K	jul-cc-pVDZ	-1.98	19.15	-21.12	-1.98	18.51	-19.58	-0.58	21.22	-20.30	0.85
M06-2X	ma-TZVP	-2.04	20.37	-22.42	-2.04	19.40	-20.22	0.02	20.69	-20.66	0.70
M08-HX	ma-TZVP	-1.02	19.82	-20.84	-1.02	19.37	-18.83	1.30	20.53	-19.23	1.47
M08-SO	ma-TZVP	-3.27	19.21	-22.48	-3.27	18.82	-20.48	-0.89	20.16	-21.00	0.54
M05-2X	ma-TZVP	-2.90	20.54	-23.44	-2.90	19.28	-20.90	-0.85	20.51	-21.29	0.73
MN12-SX	ma-TZVP	-2.06	17.27	-19.33	-2.06	16.98	-17.71	-0.08	18.23	-18.22	1.74
MN12-L	ma-TZVP	-1.51	15.40	-16.91	-1.51	15.50	-15.23	0.82	16.73	-15.69	3.32
MN15-L	ma-TZVP	-4.76	15.94	-20.70	-4.76	15.57	-18.32	-2.03	16.67	-18.67	2.24
MPW1K	ma-TZVP	-0.81	19.16	-19.97	-0.81	18.53	-18.48	0.47	21.15	-19.17	1.59
CCSD(T)-F12	jul-cc-PVTZ	-3.19	19.73	-22.92	-2.04	18.19	-20.23	-1.33	19.30	-20.63	0.00

All the energies are with ZPEs excluded and calculated using the structures optimized by M08-HX/ma-TZVP method.

Table S5 Classical forward barrier heights (V_f^\ddagger) and classical reaction energies (ΔV) (kcal/mol) of B1-B3 addition reactions.^a

Reaction	V_f^\ddagger			ΔV		
	Huang et al. ^b	This work ^c	This work ^d	Huang et al. ^b	This work ^c	This work ^d
add- <i>ipso</i>	-1.99	-1.61	-1.59	-14.68	-19.43	-19.87
add- <i>o</i>	-1.90	-0.17	-0.60	-13.49	-17.65	-17.36
add- <i>m</i>	-1.54	0.22	-0.25	-14.23	-17.98	-17.60

^aAll energies include scaled ZPEs.

^b Calculated by the B3LYP/6-311++G(2df,2pd)//B3LYP/6-31G(d,p) method by Huang et. al.¹¹

^c Calculated by the M08-SO/ma-TZVP method.

^d Calculated by the CCSD(T)-F12b/jul-cc-pVTZ//M08-HX/ma-TZVP method.

Table S6 Multi-structural torsional anharmonicity factors $F^{\text{MS-T},\alpha}$ for reactants, transition states and products of hydrogen abstraction reactions A1-A3 at selected temperatures by M08-HX/jul-cc-pVDZ method.

T(K)	$F^{\text{MS-T,Reactants}}$	$F^{\text{MS-T,TS}}$		$F^{\text{MS-T,Products}}$			
		abs-methyl	abs- <i>o</i>	abs- <i>m</i>	abs-methyl	abs- <i>o</i>	abs- <i>m</i>
220	1.167	2.592	2.298	1.905	1.031	1.197	1.147
260	1.194	2.852	2.300	1.866	1.046	1.219	1.162
298	1.213	3.073	2.284	1.823	1.059	1.233	1.169
320	1.222	3.189	2.269	1.797	1.067	1.238	1.171
350	1.231	3.333	2.244	1.760	1.077	1.242	1.172
400	1.239	3.538	2.192	1.697	1.093	1.242	1.167
500	1.238	3.829	2.069	1.572	1.118	1.223	1.144
600	1.219	3.992	1.934	1.455	1.134	1.189	1.110
700	1.190	4.059	1.798	1.347	1.143	1.147	1.071
800	1.156	4.058	1.666	1.248	1.146	1.103	1.029
900	1.118	4.009	1.543	1.157	1.144	1.058	0.987
1000	1.080	3.929	1.427	1.075	1.139	1.013	0.946
1200	1.005	3.717	1.225	0.931	1.122	0.931	0.870
1400	0.935	3.479	1.056	0.811	1.100	0.858	0.802
1600	0.872	3.242	0.916	0.711	1.077	0.793	0.743
1800	0.816	3.018	0.800	0.627	1.052	0.737	0.690
2000	0.765	2.811	0.704	0.557	1.028	0.687	0.644
2300	0.699	2.536	0.588	0.470	0.993	0.624	0.585
2500	0.660	2.374	0.525	0.423	0.971	0.587	0.551
2800	0.609	2.161	0.448	0.364	0.940	0.539	0.507
3000	0.579	2.035	0.405	0.331	0.920	0.512	0.481

Table S7 Multi-structural torsional anharmonicity factors $F^{\text{MS-T},\alpha}$ for reactants, transition states and products of additional reactions B1-B3 at selected temperatures by M08-SO/ma-TZVP method.

T(K)	$F^{\text{MS-T,Reactants}}$	$F^{\text{MS-T,TS}}$			$F^{\text{MS-T,Products}}$		
		add- <i>ipso</i>	add- <i>o</i>	add- <i>m</i>	add- <i>ipso</i>	add- <i>o</i>	add- <i>m</i>
220	1.156	2.148	2.304	2.406	2.274	1.230	2.009
260	1.183	2.241	2.363	2.491	2.354	1.205	1.975
298	1.202	2.331	2.400	2.548	2.428	1.177	1.948
320	1.210	2.382	2.414	2.572	2.470	1.161	1.936
350	1.218	2.450	2.425	2.595	2.526	1.138	1.921
400	1.226	2.553	2.424	2.611	2.616	1.101	1.903
500	1.223	2.717	2.369	2.579	2.775	1.031	1.876
600	1.203	2.820	2.271	2.493	2.898	0.968	1.847
700	1.173	2.868	2.153	2.381	2.982	0.908	1.810
800	1.137	2.873	2.027	2.256	3.030	0.853	1.763
900	1.099	2.847	1.903	2.129	3.046	0.802	1.710
1000	1.060	2.797	1.785	2.006	3.037	0.754	1.652
1200	0.985	2.658	1.570	1.778	2.965	0.670	1.531
1400	0.915	2.494	1.388	1.581	2.850	0.598	1.411
1600	0.852	2.326	1.234	1.412	2.713	0.536	1.299
1800	0.796	2.165	1.104	1.268	2.569	0.484	1.197
2000	0.746	2.014	0.994	1.146	2.426	0.439	1.104
2300	0.680	1.809	0.859	0.994	2.222	0.383	0.983
2500	0.642	1.688	0.784	0.909	2.096	0.352	0.912
2800	0.592	1.527	0.690	0.803	1.922	0.312	0.820
3000	0.563	1.432	0.637	0.742	1.817	0.289	0.766

Table S8 The calculated HPL rate constants for A1-A3 hydrogen abstraction reactions in $\text{cm}^3\text{molecule}^{-1}\text{s}^{-1}$.

T(K)	Forward rate constants			Reverse rate constants		
	abs-methyl	abs- <i>o</i>	abs- <i>m</i>	abs-methyl	abs- <i>o</i>	abs- <i>m</i>
220	7.49E-13	3.80E-16	2.72E-16	1.66E-41	5.82E-23	1.07E-22
260	7.43E-13	1.32E-15	9.42E-16	3.81E-37	1.64E-21	2.66E-21
298	8.12E-13	3.33E-15	2.39E-15	4.76E-34	1.79E-20	2.69E-20
320	8.71E-13	5.24E-15	3.78E-15	1.40E-32	5.60E-20	8.12E-20
350	9.69E-13	9.00E-15	6.56E-15	7.22E-31	2.14E-19	2.98E-19
400	1.17E-12	1.92E-14	1.42E-14	1.44E-28	1.32E-18	1.76E-18
500	1.70E-12	5.99E-14	4.59E-14	2.61E-25	1.85E-17	2.33E-17
600	2.36E-12	1.39E-13	1.09E-13	4.12E-23	1.17E-16	1.43E-16
700	3.19E-12	2.68E-13	2.16E-13	1.61E-21	4.69E-16	5.60E-16
800	4.17E-12	4.57E-13	3.77E-13	2.62E-20	1.40E-15	1.65E-15
900	5.34E-12	7.19E-13	6.07E-13	2.37E-19	3.40E-15	4.01E-15
1000	6.70E-12	1.06E-12	9.14E-13	1.42E-18	7.17E-15	8.47E-15
1200	1.01E-11	2.00E-12	1.80E-12	2.21E-17	2.35E-14	2.80E-14
1400	1.43E-11	3.32E-12	3.10E-12	1.69E-16	5.89E-14	7.10E-14
1600	1.96E-11	5.04E-12	4.86E-12	8.08E-16	1.23E-13	1.50E-13
1800	2.58E-11	7.16E-12	7.10E-12	2.84E-15	2.27E-13	2.81E-13
2000	3.31E-11	9.71E-12	9.86E-12	7.98E-15	3.81E-13	4.77E-13
2300	4.61E-11	1.43E-11	1.49E-11	2.80E-14	7.29E-13	9.25E-13
2500	5.63E-11	1.78E-11	1.90E-11	5.60E-14	1.05E-12	1.35E-12
2800	7.38E-11	2.39E-11	2.60E-11	1.35E-13	1.70E-12	2.20E-12
3000	8.70E-11	2.84E-11	3.12E-11	2.23E-13	2.24E-12	2.92E-12

Table S9 The calculated HPL rate constants for B1-B3 OH-addition reactions (cm³molecule⁻¹s⁻¹ for forward reactions and s⁻¹ for reverse reactions).

T(K)	Forward rate constants			Reverse rate constants		
	add- <i>ipso</i>	add- <i>o</i>	add- <i>m</i>	add- <i>ipso</i>	add- <i>o</i>	add- <i>m</i>
220	1.04E-11	3.33E-12	6.35E-13	5.78E-06	2.25E-04	3.02E-05
260	5.18E-12	2.42E-12	5.94E-13	3.93E-03	8.83E-02	1.70E-02
298	3.36E-12	2.03E-12	5.97E-13	3.96E-01	6.10E+00	1.50E+00
320	2.79E-12	1.90E-12	6.08E-13	3.51E+00	4.54E+01	1.25E+01
350	2.30E-12	1.78E-12	6.31E-13	4.45E+01	4.71E+02	1.48E+02
400	1.84E-12	1.69E-12	6.83E-13	1.34E+03	1.09E+04	4.03E+03
500	1.49E-12	1.68E-12	8.22E-13	1.61E+05	9.12E+05	4.20E+05
600	1.42E-12	1.80E-12	9.96E-13	3.96E+06	1.78E+07	9.35E+06
700	1.45E-12	1.98E-12	1.20E-12	3.90E+07	1.50E+08	8.59E+07
800	1.54E-12	2.20E-12	1.43E-12	2.17E+08	7.40E+08	4.53E+08
900	1.68E-12	2.45E-12	1.68E-12	8.22E+08	2.57E+09	1.64E+09
1000	1.83E-12	2.74E-12	1.95E-12	2.38E+09	6.95E+09	4.61E+09
1200	2.21E-12	3.38E-12	2.56E-12	1.17E+10	3.09E+10	2.15E+10
1400	2.66E-12	4.13E-12	3.26E-12	3.63E+10	8.96E+10	6.44E+10
1600	3.17E-12	4.96E-12	4.03E-12	8.44E+10	1.99E+11	1.46E+11
1800	3.73E-12	5.88E-12	4.88E-12	1.62E+11	3.69E+11	2.74E+11
2000	4.34E-12	6.89E-12	5.79E-12	2.74E+11	6.05E+11	4.54E+11
2300	5.36E-12	8.57E-12	7.32E-12	5.03E+11	1.08E+12	8.16E+11
2500	6.10E-12	9.78E-12	8.42E-12	6.94E+11	1.47E+12	1.11E+12
2800	7.30E-12	1.18E-11	1.02E-11	1.03E+12	2.15E+12	1.63E+12
3000	7.94E-12	1.32E-11	1.15E-11	1.25E+12	2.65E+12	2.01E+12

Table S10 High-pressure-limit rate constants ($k \times 10^{11}$ cm³mole⁻¹s⁻¹) of addition reactions and overall reactions at 298 K.

	Pan and Wang ¹² (2015)	This work ^a	Expt.
$k_{\text{add}}^{\text{b}}$	0.176 ^c / 5.24 ^d	0.598 0.680	$\sim 1.22 \pm 0.19^{\text{f}}$ $\sim 1.143 \pm 0.34^{\text{g}}$ $\sim 1.19 \pm 0.07^{\text{h}}$
$k_{\text{all}}^{\text{e}}$			

^a Our MS-CVT/SCT results based on M08-SO/ma-TZVP PESs;

^b Total rate constant of addition reactions (B1-B3);

^c TST result of Pan and Wang¹² based on M06-2X/6-311++G (2df, 2p) PESs;

^d TST result of Pan and Wang¹² based on ROCBS-QB3 PESs;

^e Total rate constant of H-abstraction (A1-A3) reactions and addition (B1-B3) reactions;

^f Atkinson et al.¹³ at 1 atm and 296 ± 2 K in the air;

^g Anderson et al.¹⁴ at 760 Torr and room temperature in the air;

^h Mehta et al.¹⁵ at 8.0-8.1 Torr with He as bath gas.

Table S11 The total rate constants of additional reactions (the sum of B1-B3 channels) under several selected pressures with He as the bath gas in $\text{cm}^3\text{molecule}^{-1}\text{s}^{-1}$.

T(K)	8 Torr	10 Torr	20 Torr	100 Torr	1 atm	10 atm	100 atm	500 atm
220	1.42E-11	1.43E-11	1.43E-11	1.44E-11	1.44E-11	1.44E-11	1.44E-11	1.44E-11
260	7.94E-12	7.99E-12	8.09E-12	8.17E-12	8.19E-12	8.19E-12	8.20E-12	8.20E-12
298	5.46E-12	5.54E-12	5.73E-12	5.93E-12	5.98E-12	5.99E-12	5.99E-12	5.99E-12
320	4.52E-12	4.63E-12	4.89E-12	5.19E-12	5.28E-12	5.30E-12	5.30E-12	5.30E-12
350	3.50E-12	3.64E-12	4.00E-12	4.49E-12	4.68E-12	4.71E-12	4.71E-12	4.71E-12
400	2.14E-12	2.29E-12	2.74E-12	3.59E-12	4.08E-12	4.20E-12	4.21E-12	4.21E-12
500	5.29E-13	6.02E-13	8.76E-13	1.76E-12	3.01E-12	3.80E-12	3.98E-12	4.00E-12
600	7.80E-14	9.31E-14	1.58E-13	4.79E-13	1.42E-12	2.98E-12	3.95E-12	4.15E-12
700	8.30E-15	1.02E-14	1.91E-14	7.68E-14	3.64E-13	1.43E-12	3.21E-12	4.12E-12
800	7.55E-16	9.40E-16	1.85E-15	8.65E-15	5.53E-14	3.63E-13	1.55E-12	2.99E-12
900	6.40E-17	8.00E-17	1.60E-16	7.88E-16	5.76E-15	5.07E-14	3.62E-13	1.12E-12
1000	4.92E-18	6.15E-18	1.23E-17	6.15E-17	4.65E-16	4.55E-15	4.21E-14	1.82E-13
1200	1.65E-20	2.07E-20	4.14E-20	2.07E-19	1.57E-18	1.57E-17	1.57E-16	7.84E-16
1400	2.74E-23	3.42E-23	6.84E-23	3.42E-22	2.60E-21	2.60E-20	2.60E-19	1.30E-18
1600	3.26E-26	4.08E-26	8.16E-26	4.08E-25	3.10E-24	3.10E-23	3.10E-22	1.55E-21
1800	3.83E-29	4.78E-29	9.56E-29	4.78E-28	3.63E-27	3.63E-26	3.63E-25	1.82E-24
2000	5.05E-32	6.31E-32	1.26E-31	6.31E-31	4.80E-30	4.80E-29	4.80E-28	2.40E-27
2300	3.63E-36	4.53E-36	9.06E-36	4.53E-35	3.44E-34	3.44E-33	3.44E-32	1.72E-31
2500	8.37E-39	1.05E-38	2.09E-38	1.05E-37	7.95E-37	7.95E-36	7.95E-35	3.98E-34
2800	1.46E-42	1.82E-42	3.65E-42	1.82E-41	1.39E-40	1.39E-39	1.39E-38	6.93E-38
3000	6.08E-45	7.60E-45	1.52E-44	7.60E-44	5.77E-43	5.77E-42	5.77E-41	2.89E-40

Table S12 The total rate constants of additional reactions (the sum of B1-B3 channels) under several selected pressures with Ar as the bath gas in $\text{cm}^3\text{molecule}^{-1}\text{s}^{-1}$.

T(K)	8 Torr	10 Torr	20 Torr	100 Torr	1 atm	10 atm	100 atm	500 atm
220	1.43E-11	1.43E-11	1.43E-11	1.44E-11	1.44E-11	1.44E-11	1.44E-11	1.44E-11
260	8.01E-12	8.04E-12	8.12E-12	8.18E-12	8.19E-12	8.19E-12	8.20E-12	8.20E-12
298	5.59E-12	5.65E-12	5.80E-12	5.94E-12	5.98E-12	5.99E-12	5.99E-12	5.99E-12
320	4.70E-12	4.79E-12	5.00E-12	5.22E-12	5.29E-12	5.30E-12	5.30E-12	5.30E-12
350	3.74E-12	3.86E-12	4.16E-12	4.55E-12	4.69E-12	4.71E-12	4.71E-12	4.71E-12
400	2.42E-12	2.57E-12	3.00E-12	3.74E-12	4.12E-12	4.20E-12	4.21E-12	4.21E-12
500	6.87E-13	7.76E-13	1.10E-12	2.06E-12	3.23E-12	3.86E-12	3.99E-12	4.00E-12
600	1.14E-13	1.35E-13	2.25E-13	6.42E-13	1.73E-12	3.27E-12	4.04E-12	4.18E-12
700	1.27E-14	1.56E-14	2.89E-14	1.12E-13	4.99E-13	1.77E-12	3.53E-12	4.27E-12
800	1.21E-15	1.50E-15	2.94E-15	1.36E-14	8.39E-14	5.12E-13	1.95E-12	3.43E-12
900	1.04E-16	1.30E-16	2.60E-16	1.28E-15	9.24E-15	7.89E-14	5.24E-13	1.50E-12
1000	8.07E-18	1.01E-17	2.02E-17	1.01E-16	7.60E-16	7.39E-15	6.68E-14	2.77E-13
1200	2.71E-20	3.39E-20	6.78E-20	3.39E-19	2.58E-18	2.58E-17	2.57E-16	1.28E-15
1400	4.46E-23	5.58E-23	1.12E-22	5.58E-22	4.24E-21	4.24E-20	4.24E-19	2.12E-18
1600	5.30E-26	6.63E-26	1.33E-25	6.63E-25	5.04E-24	5.04E-23	5.04E-22	2.52E-21
1800	6.19E-29	7.73E-29	1.55E-28	7.73E-28	5.88E-27	5.88E-26	5.88E-25	2.94E-24
2000	8.14E-32	1.02E-31	2.04E-31	1.02E-30	7.73E-30	7.73E-29	7.73E-28	3.87E-27
2300	5.82E-36	7.27E-36	1.45E-35	7.27E-35	5.53E-34	5.53E-33	5.53E-32	2.76E-31
2500	1.34E-38	1.67E-38	3.35E-38	1.67E-37	1.27E-36	1.27E-35	1.27E-34	6.36E-34
2800	2.33E-42	2.91E-42	5.82E-42	2.91E-41	2.21E-40	2.21E-39	2.21E-38	1.11E-37
3000	9.68E-45	1.21E-44	2.42E-44	1.21E-43	9.19E-43	9.19E-42	9.19E-41	4.60E-40

Table S13 The overall rate constants ($k \times 10^{12} \text{ cm}^3 \text{mole}^{-1} \text{s}^{-1}$) at 298 K, 320 K, and 800 K under the same or similar pressure conditions.

T	298 K		320 K		800 K
	p	100 Torr	1 atm	100 Torr	1 atm
This work (He)		6.74	6.80	6.07	6.16
This work (Ar)		6.76	6.80	6.10	6.17
		15.3±1.5			
Hansen et al. ¹⁶		(101 Torr)			
Perry et al. ¹⁷		14.3±1.5		14.0±1.5	
Nicovich et al. ¹⁸			14.2±1.7 (800 Torr)		15.8±1.8 (800 Torr)
Anderson et al. ¹⁴			11.43±0.34		
Atkinson et al. ¹³			12.2±1.9		(800 Torr, 757K)

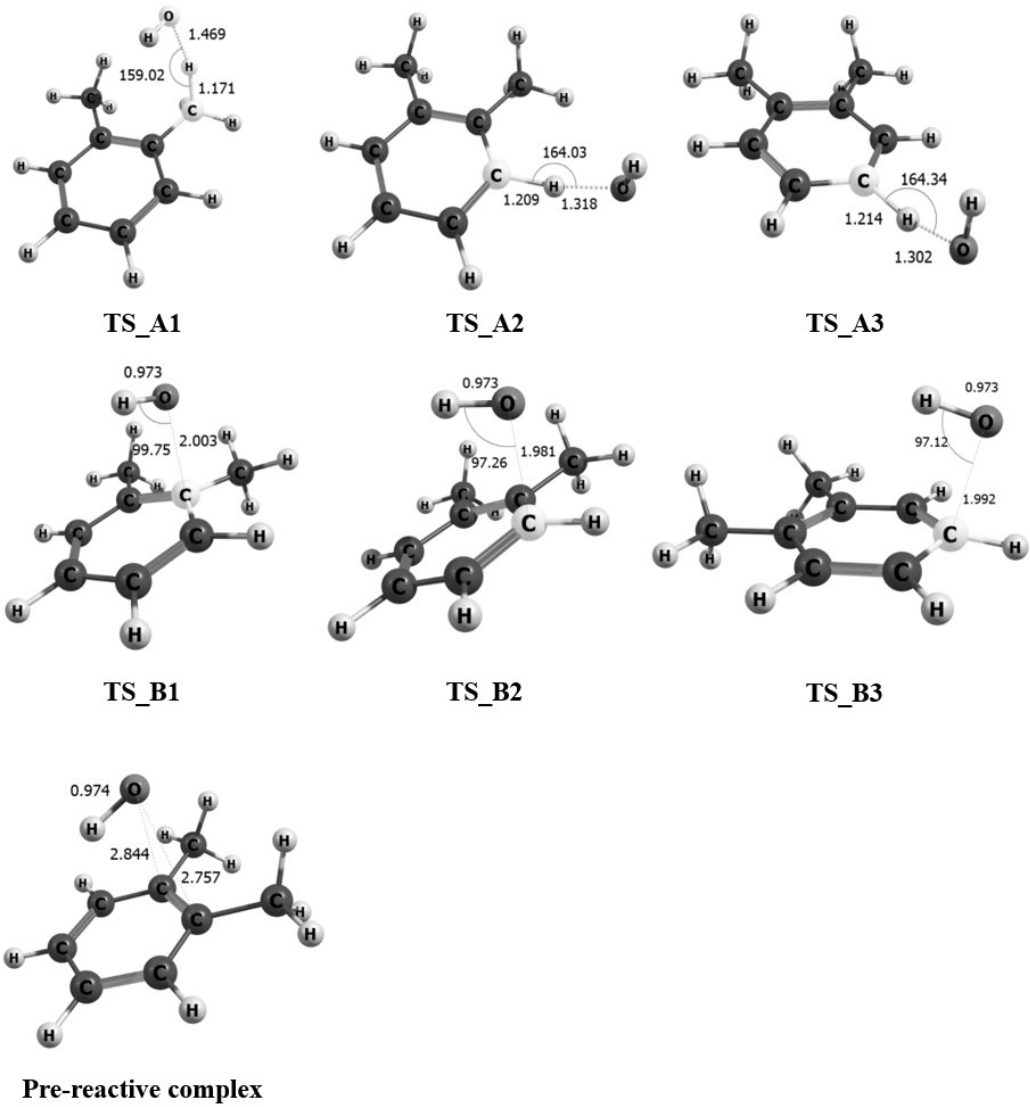


Fig. S1 The optimized lowest-energy transition state structures of *o*-xylene reactions with OH for A1-A3 channels by M08-HX/jul-cc-pVDZ method, and for B1-B3 channels by M08-SO/ma-TZVP method. The structure of the pre-reactive complex is optimized by M08-HX/ma-TZVP method. Bond distances are given in Å.

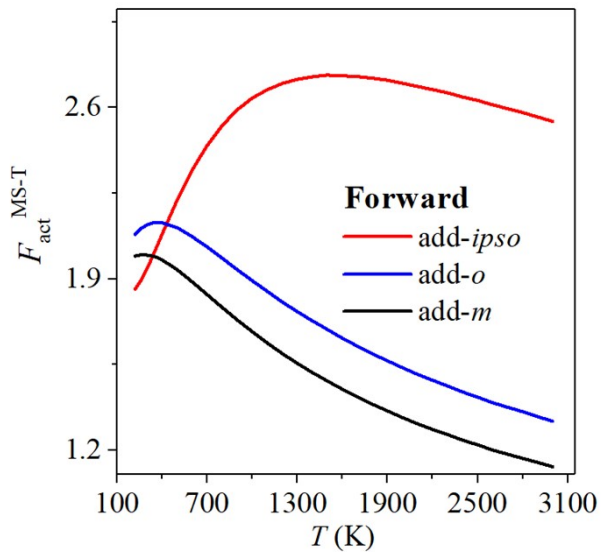
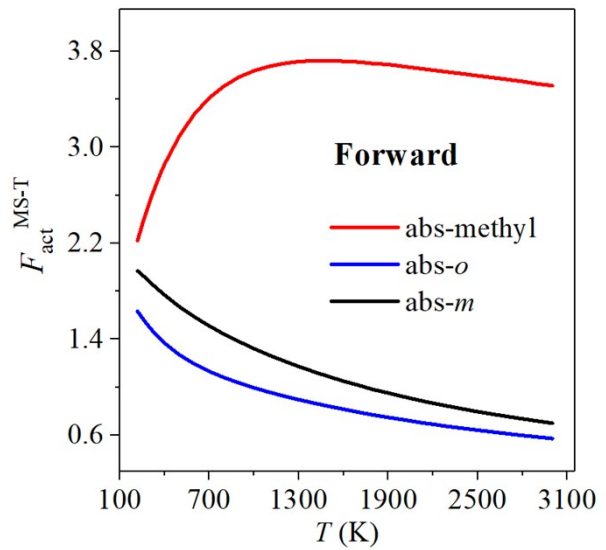


Fig. S2 The multi-structural anharmonicity factor $F_{\text{act}}^{\text{MS-T}}$ for hydrogen abstraction and addition reactions.

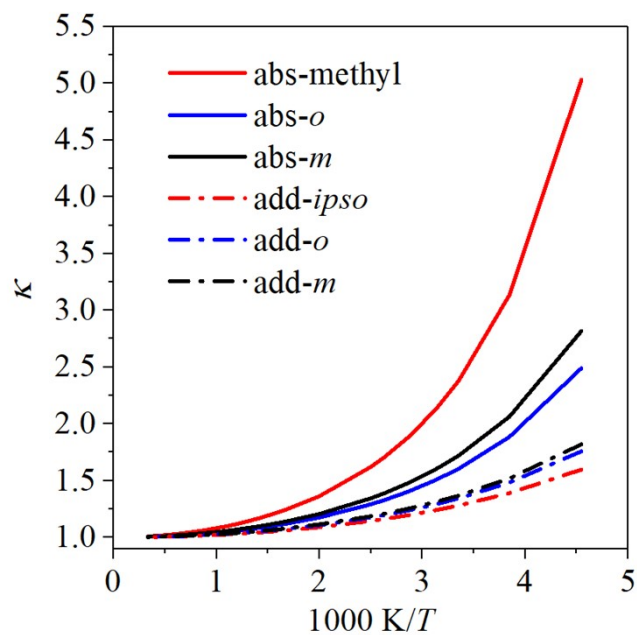


Fig. S3 Small-curvature tunneling transmission coefficients (κ^{SCT}) for A1-A3 and B1-B3 reactions in the high-pressure limit. Straight and dash-dot lines represent results for hydrogen abstraction reactions by M08-HX/jul-cc-pVDZ and addition reactions by M08-SO/ma-TZVP, respectively.

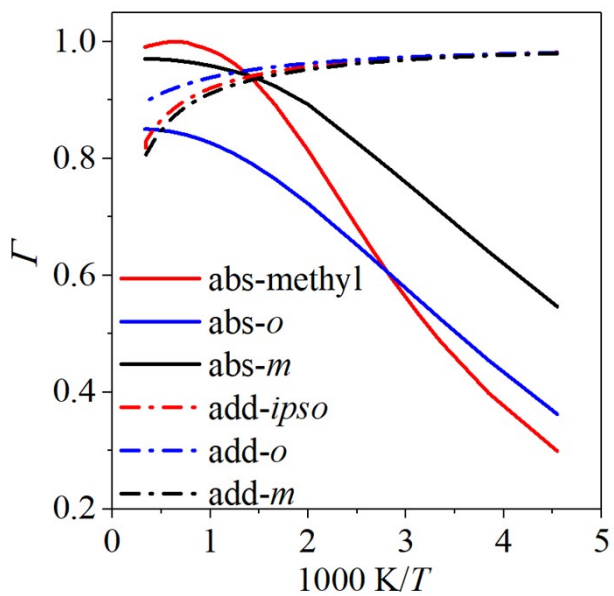


Fig. S4 Reccrossing transmission coefficients (Γ^{CVT}) for A1-A3 and B1-B3 reactions. Straight and dash-dot lines represent results for hydrogen abstraction reactions by M08-HX/jul-cc-pVDZ and addition reactions by M08-SO/ma-TZVP, respectively.

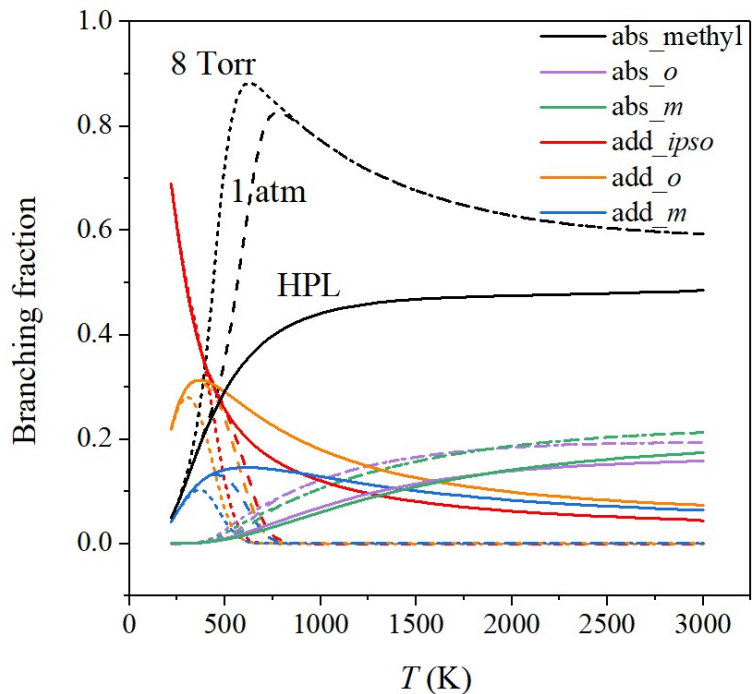


Fig. S5 Branching fractions of six reaction channels with the bath gas of He. The dot lines, dash lines and solid lines represent the branching fractions under the pressure condition of 8 torr, 1 atm and HPL, respectively.

References

1. I. M. Alecu, J. Zheng, Y. Zhao and D. G. Truhlar, *J. Chem. Theory Comput.*, 2010, **6**, 2872-2887.
2. L. G. Gao, J. Zheng, A. Fernández-Ramos, D. G. Truhlar and X. Xu, *J. Am. Chem. Soc.*, 2018, **140**, 2906-2918.
3. J. Zheng, R. Meana-Pañeda and D. G. Truhlar, *J. Am. Chem. Soc.*, 2014, **136**, 5150-5160.
4. R. M. Zhang, D. G. Truhlar and X. Xu, *Research (Washington)*, 2019, **2019**, 1-19.
5. J. Bloino, M. Biczysko and V. Barone, *J. Chem. Theory Comput.*, 2012, **8**, 1015-1036.
6. K. M. Kuhler, D. G. Truhlar and A. D. Isaacson, *J. Chem. Phys.*, 1996, **104**, 4664-4671.
7. H. H. Nielsen, *The Vibration-rotation Energies of Molecules and their Spectra in the Infra-red* , Springer-Verlag OHG, Berlin · Göttingen · Heidelberg, 1959.
8. Q. Zhang, P. N. Day and D. G. Truhlar, *J. Chem. Phys.*, 1993, **98**, 4948-4958.
9. I. M. Mills, *Vibration-Rotation Structure in Asymmetric- and Symmetric-Top Molecules*, Academic: New York, 1972.
10. B. J. Lynch, P. L. Fast, M. Harris and D. G. Truhlar, *J. Phys. Chem. A*, 2000, **104**, 4811-4815.
11. M. Huang, W. Zhang, Z. Wang, L. Hao, W. Zhao, X. Liu, B. Long and L. Fang, *Int. J. Quantum Chem.*, 2008, **108**, 954-966.
12. S.-S. Pan and L.-M. Wang, *Acta Physico-Chimica Sinica*, 2015, **31**, 2259-2268.
13. R. Atkinson and S. M. Aschmann, *Int. J. Chem. Kinet.*, 1989, **21**, 355-365.
14. R. S. Anderson, E. Czuba, D. Ernst, L. Huang, A. E. Thompson and J. Rudolph, *J. Phys. Chem. A*, 2003, **107**, 6191-6199.
15. D. Mehta, A. Nguyen, A. Montenegro and Z. Li, *J. Phys. Chem. A*, 2009, **113**, 12942-12951.
16. D. A. Hansen, R. Atkinson and J. N. Pitts Jr, *J. Phys. Chem.*, 1975, **79**, 1763-1766.
17. R. A. Perry, R. Atkinson and J. N. Pitts Jr, *J. Phys. Chem.*, 1977, **81**, 296-304.
18. J. M. Nicovich, R. L. Thompson and A. R. Ravishankara, *J. Phys. Chem.*, 1981, **85**, 2913-2916.